JOURNAL OF MATERIALS SCIENCE 35 (2000) 5667–5672

The critical length of the hydride cluster in delayed hydride cracking of Zr-2.5wt% Nb

D. YAN, R. L. EADIE
Department of Chemical and Materials Engineering, University of Alberta, Edmonton, Alberta, Canada T6G 2G6
E-mail: Reg.Eadie@ualberta.ca

In delayed hydride cracking (DHC) of Zr-2.5wt% Nb alloy, the hydride cluster at the crack tip has a critical length, which is a function of the stress intensity factor K_I and other parameters. When $K_I > K_{IH}$, the threshold stress intensity factor, the hydride cluster must grow to this critical length before it will fracture. On the other hand, when $K_I < K_{IH}$, there is a maximum length to which the hydride cluster can grow, and this length is insufficient for fracture *i.e.* less than the critical length. In this work, the lengths of the hydride cluster were experimentally studied for $K_I < K_{IH}$ and $K_I > K_{IH}$ near K_{IH}. A modified experimental method was used, that permitted the hydride clusters to be formed and fractured individually. The hydride clusters were observed to be wedge-shaped, in agreement with the predictions by Metzger and Sauvé (PVP, vol. 326, ASME, 1996). The lengths of hydride cluster measured in this work are compared with existing theoretical predictions. A good general agreement was obtained, but some differences are discussed.

1. Introduction

The delayed hydride cracking (DHC) in Zr-2.5wt% Nb alloy has been of research interest for decades. This alloy is the major structural material for the pressure tubes of the primary heat transport system in CANDU (Canadian Deuterium Uranium) nuclear reactors. In general, DHC has been accepted as a repeated process that involves stress-induced hydrogen diffusion, hydride precipitation and fracturing of the hydrided crack tip region [1]. When the applied stress intensity factor is sufficient, the hydride cluster at the crack tip fractures when it has reached a certain length, which is regarded as the critical length for fracture [1]. For small stress intensity factors, which are below the threshold for DHC, the hydride cluster at the crack tip will not fracture but there is a maximum length to which the cluster will grow [2, 3]. The critical length for fracture and the maximum growth length are a function of the stress intensity factor and other parameters, such as the diffusible hydrogen concentration, the yield strength *etc*. [2–5].

The critical length for hydride fracture at $K_I > K_{IH}$ is an important factor in studying the critical conditions for DHC, and the variation of the length with the stress intensity factor K_I has been theoretically studied [2, 4, 5]. Shi and Puls [2] assumed a critical stress model for hydride fracture and, by using both analytical and numerical methods, calculated the critical length for fracture of hydride as a function of K_I. They showed that as $K_I (K_I > K_{IH})$ decreases, this critical length will increase, and when K_I drops near K_{IH}, there is a sharp increase in the hydride length for fracture. In an alternative analysis, using an energy balance model, Zheng *et al*. [4] predicted a similar relation. In their work, based on numerical analysis, an explicit expression (Equation 8 of [4]) for the critical hydride length vs. K_I was given. In a more recent work by Zheng *et al*. [5], a combined stress and energy model was proposed, and used to explain the critical hydride lengths in their respective valid ranges. The maximum length to which the hydride can grow [2, 3], is for the cases when $K_I < K_{IH}$. By using a moving boundary diffusion model based on the interaction between the hydrostatic stress field and hydrogen concentration gradient, Shi and Puls [2] gave an expression for the maximum hydride length L_{max} as a function of K_I and the hydrogen concentration in the specimen. Their expression shows $L_{max} \propto K_I^2$. Using a finite element method program, Metzger *et al*. [3] took into account the volume dilation caused by hydride formation and its effect on the stress field and therefore hydrogen diffusion at the crack tip. They predicted the self-limiting process of hydride growth and a wedge-shaped hydride at crack tip, which they also observed experimentally.

There was other experimental work on this issue [6, 7] in which measurements of the DHC striation spacing on the fracture surface were made at various K_I and/or temperatures. The K_I used in these works were large ones with K_I larger than K_{IH}, and in stage II of the DHC velocity vs. K_I curve [6]. The measured striation spacing showed a similar but more gradual dependency on K_I [7] than the critical length for hydride fracture predicted by theoretical work. For notched specimens, hydride length and thickness were measured at different normal stresses below the threshold for hydride fracture [8]. Very little systematic experimental work has been conducted to study the hydride length for the cases

when $K_I < K_{IH}$, or for the near-K_{IH} region, i.e. stage I, and to compare with existing theoretical work. In this work, experiments were conducted to measure the maximum length for hydride growth for $K_I < K_{IH}$, as well as the critical hydride length for the cases $K_I > K_{IH}$ but near K_{IH} (stage I). This information will help us better understand the K_{IH} phenomenon.

The striation method is not applicable to studying the hydride lengths when $K_I < K_{IH}$, and in this work, a modified experimental method was developed. In this modified method, the specimens were fatigued between consecutive experiments, so that the hydride clusters in each DHC experiment were separated, and can thus be observed and studied individually.

2. Experimental

The Chalk River Laboratory (CRL) of Atomic Energy of Canada Ltd. (AECL) provided the Zr-2.5wt% Nb alloy used in this work. These samples are from different pressure tubes but have very similar characteristics. The composition is given in Table I. The microstructures of the alloy mainly consisted of α and β phases in the proportion 92% to 8%. The texture of similar pressure tube materials had been measured [9]. The fractions of basal pole normals in radial, circumferential and axial directions for this material were 0.32, 0.62 and 0.06 with only small variations. The circumferential tensile properties were measured in this work, and are given in Table II. The Vickers hardness for these specimens was about 226 (HV10).

Tapered double cantilever beam specimens (constant-K_I specimen) were used for the experiments. The specimens were electrolytically hydrided and diffusion-annealed at 400°C, and were then machined by electric discharge machining (EDM). The hydrogen level in the specimens was 165 μg/g. The specimens were so cut that the cracking was on the axial-radial plane. A more detailed description of the preparation is given in [10]. To obtain a sharp crack tip, the specimens were fatigue pre-cracked using decreasing ΔK_I. The maximum K_I used during the finishing stage of fatigue pre-cracking was about 2.0 MPa$\sqrt{}$m, and the total length of pre-crack was not less than 1.0 mm, which conforms to the ASTM standard for pre-cracking (ASTM E 1681-95).

Two testing rigs were simultaneously used for the K_{IH} experiments in this work. Rig 1 was a Tension/Compression Testing Machine, with the load being computer-controlled through a stepmotor. Rig 2 used a lever with a mechanical advantage of 10 to 1 and dead weights for loading. Loading was manual on this rig. Acoustic emission (AE) was the major technique used for monitoring cracking for both rigs, although electrical potential drop (PD) technique was also used in rig 1 [10].

Acoustic emissions were monitored in the range 0.1 to 0.3 MHz using ringdown counting at about 90 dB total amplification on Dunegan Endevco equipment. A detailed description of the AE setup is given in [10]. A dummy specimen, which was made of Zr-2.5wt% Nb alloy, neither pre-cracked nor hydrided, was used to test the noise level of the AE signal collection. For the same experiment on this dummy specimen, no appreciable AE signals (less than 50 counts) were detected. This means that when appreciable AE signals are detected, one has reason to believe that the signals come from the specimen. In this work, the AE technique was mainly used to monitor ongoing DHC or to assure that there were no cracking events. When the load was applied to the specimen, several possible factors may have contributed to the AE signals. The major one would have been the fracture of the hydride cluster (DHC) which formed at the crack tip. However, other factors also existed, such as the fracture of non-reoriented hydrides, which lay in the axial-circumferential plane. This was particularly possible when these hydrides lay close to the crack tip where the stresses are enhanced in all three principle directions under the plane strain conditions. As the crack tip advanced with DHC, these latter phenomena may have accompanied. However, if AE signals were not detected, one had reason to believe that all these processes, including DHC, have ceased in the specimen.

The temperature 150°C was chosen for the experiments, because at this temperature the effect of oxidation on the fracture surface was not obvious. The temperature was first raised to the peak temperature of 210°C, held there for 1 hour (2 hours for rig 2), and then decreased to the testing temperature of 150°C at a rate of 1–2°C/minute. Then the selected K_I was applied to the specimen. The K_I was kept constant during each experiment. The test time ranged from 40–80 hours. This waiting period was for the hydride cluster at the crack tip to grow to its maximum length or to a length long enough for fracture. When the experiment was finished, the load was first removed and then the specimen was furnace-cooled to room temperature. Between any two consecutive experiments, the specimen was fatigued to obtain a crack length increment of about 400 μm, so that the specimen started with similarly conditioned crack tips for each experiment.

Four specimens were used for the experiment, with the fifth one used as a reference for fractography study. After each experiment, a layer of about 0.1 mm was ground off one side of the specimen and that surface polished and etched to reveal any hydride clusters. This grinding was to remove the plane stress region at the specimen surface. The other side of the specimen was

TABLE I Composition of the Zr-2.5wt% Nb alloy

	Zr	Nb	Sn	Fe	Cr	Ni	Mo	O (μg/g)	H (μg/g)
Wt%	balance	2.6	0.0025	0.05	0.01	0.0035	0.0025	1200	5

TABLE II Circumferential tensile properties

Temperature (°C)	Tensile stress (MPa)	0.2% yield stress (MPa)	Elongation (%)	Area reduction (%)
25	860	830	20	71
150	695	630	20	80

never ground, so that the shape of the crack front at that side was preserved for fractography study.

Some of the specimens were opened after all the experiments had been done, mainly to see the variation of crack length in the specimen thickness direction. It was found that for specimens, which had undergone many polishings and etchings, the fracture surface was discoloured and difficult to interpret, probably because the etching solution had leaked onto the fracture surfaces. Therefore, the reference specimen was never polished or etched. Three experiments were conducted on it.

3. Results

The hydride clusters seen at the crack tip after etching usually had one of two situations. In the first case, there was only one unfractured hydride cluster seen at the crack tip. This case was for small K_I below K_{IH}. For this case, AE signals were usually detected in the early stage of the experiment, but later leveled off and stopped. The experiment was stopped after AE had stopped for at least 30–40 hours. Fig. 1 shows the typical AE signals vs. test time and the hydride cluster observed at the crack tip. In the second case, there were several fractured hydride clusters observed at the crack tip, and the

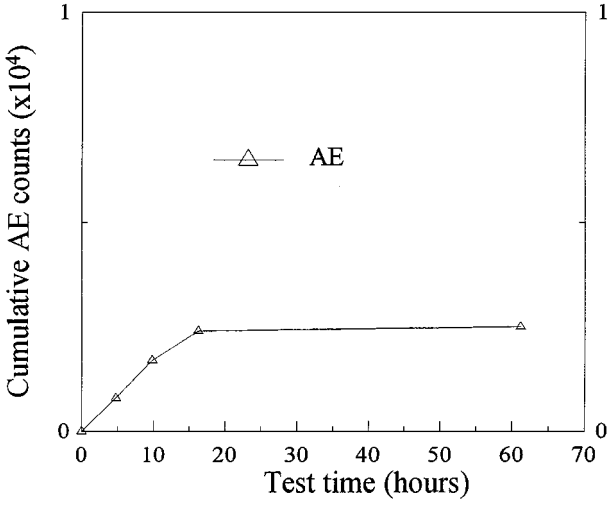

(a)

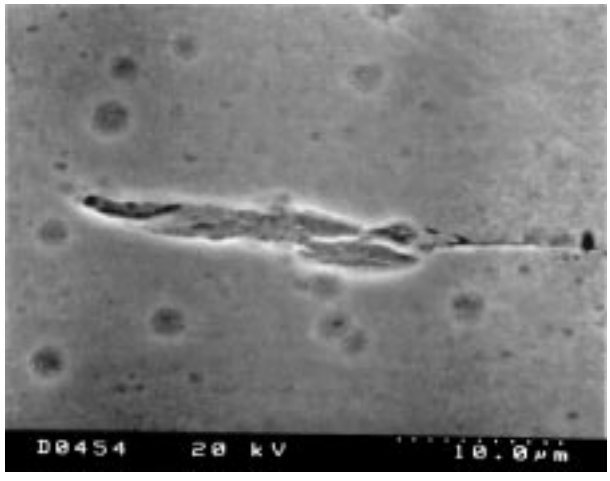

(b)

Figure 1 The unfractured hydride cluster ($K_I = 5.6$ MPa$\sqrt{}$m). (a) The AE vs. test time; (b) the hydride cluster at crack tip.

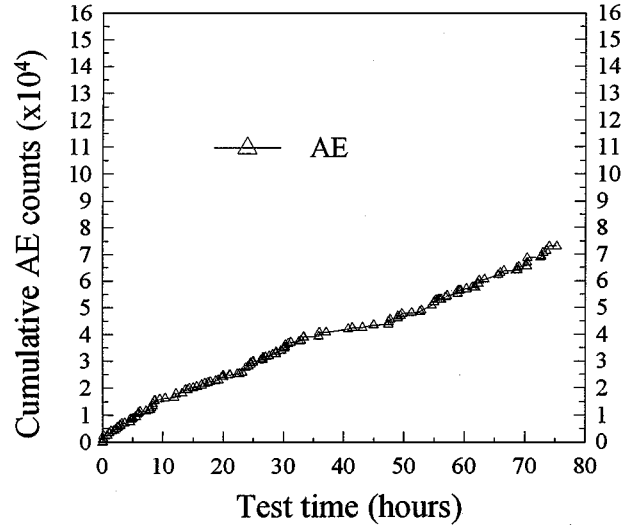

(a)

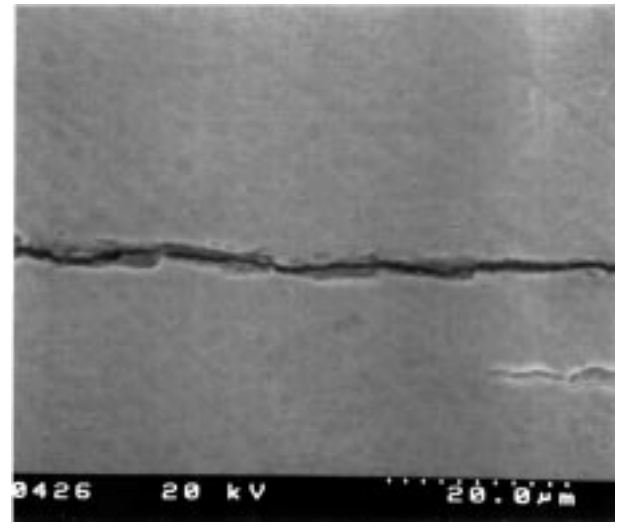

(b)

Figure 2 The fractured hydride clusters ($K_I = 7.0$ MPa$\sqrt{}$m). (a) The AE vs. test time; (b) the hydride clusters at crack tip.

AE signals observed were continuous. This was usual for K_I higher than K_{IH}. In this case, the length of the first hydride cluster was measured. Fig. 2 shows the typical AE signals vs. test time, and the hydride cluster(s) observed at crack tip. For both cases, the hydride clusters were found to have a wedge shape, which is in agreement with the hydride shape predicted by Metzger and Sauvé [3].

Fig. 3 summarizes the hydride cluster lengths measured at different applied K_I. At low K_I, those clusters were unfractured, and the cluster length was the maximum to which the cluster will grow for that K_I. In Fig. 3, it is fit by the dotted line, which is proportional to K_I^2. The dotted line is $L = \frac{2.19}{\pi}(K_I)^2$, where L is the cluster length in μm, K_I is the applied stress intensity factor in MPa$\sqrt{}$m. For these small K_I, this length is insufficient for fracture. At higher K_I, the solid line gives the length of the (first) hydride cluster that fractured. In Fig. 3, one sees that as K_I increases, the observed hydride cluster length first increases for low K_I and then reverses direction when K_I exceeds 6.0 MPa$\sqrt{}$m. However, no hydride cluster was observed at the crack

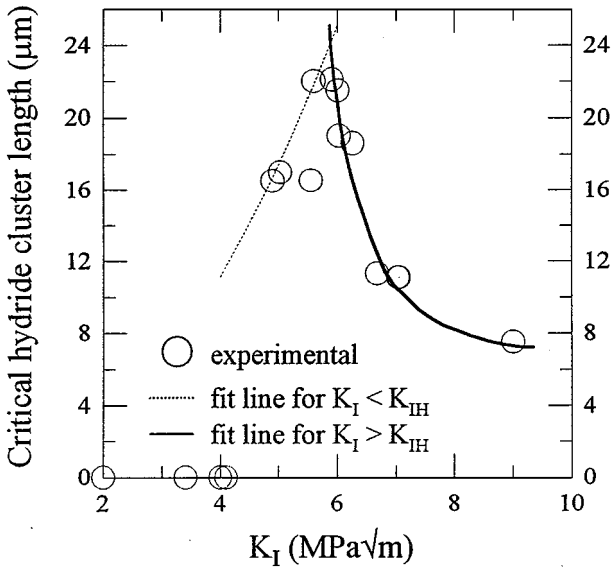

Figure 3 The critical hydride cluster lengths measured.

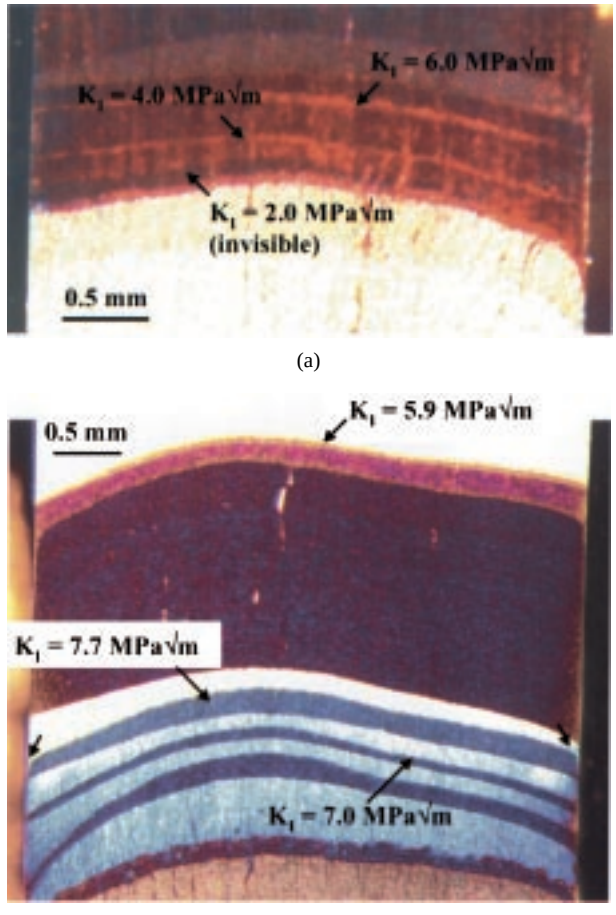

Figure 4 Fracture surface showing variation of crack length along specimen thickness direction: (a) A specimen with many polishings and etchings; (b) a specimen with no polishing and etching.

tip for $K_I \leq 4.0$ MPa$\sqrt{\text{m}}$, even if the specimen was ground to its mid-thickness. Based on the magnitude of the hydrostatic stress at the crack tip, there should be sufficient stress for hydride formation, but no hydride is observed. The reason for this is still not clear.

Fig. 4 shows the variation of crack length along the specimen thickness. Fig. 4a and b give the fracture surfaces of a polished and etched specimen and the reference specimen that had never been polished or etched, respectively. Arrows mark the crack regions, corresponding to the experiments for this work. In Fig. 4a the fracture surface was difficult to interpret, probably due to the etching processes. In Fig. 4b the crack regions corresponding to the three experiments are more clearly defined on the fracture surface. From Fig. 4, one can see that:

(i) the crack front curves in general towards the cracking direction in the middle of specimen;

(ii) the crack length is slightly longer close to the middle of specimen thickness than close to the specimen side surfaces. But for $K_I \leq 7.0$ MPa$\sqrt{\text{m}}$, the K_I range in which we did most of the experiments, the variation of crack length along the specimen thickness is small.

(iii) unbroken matrix ligaments can be seen close to the specimen side surfaces, especially in Fig. 4b, as marked by arrows. The thickness of the unbroken matrix ligaments is about 10–20 μm in the specimen thickness direction. This means that grinding 100 μm off the specimen side surface is more than enough to show the crack length "inside" the specimen.

4. Discussion

In Fig. 3, the dotted-line shows that the growth of the hydride cluster is limited to some value, which increases as K_I increases, and the solid line shows that the critical length for fracture of a hydride cluster increases as K_I decreases. Different physical processes are involved here.

The hydride growth limit is controlled by two factors. One is the interaction between the hydrostatic stress gradient and the hydrogen concentration gradient [2, 3], and the other is the effect of volume dilation caused by hydride formation on the hydrostatic stress [3]. The hydrostatic stress gradient near the crack tip provides the driving force for hydrogen diffusion. This driving force would decrease, as the hydrogen diffusion builds up a concentration gradient in the opposite direction to the hydrostatic stress gradient [2]. This gradient build-up does not occur here since by cooling from well above the test temperature the hydrogen concentration has been increased all across the specimen to the precipitation *solvus* and cannot increase further without precipitation. The force for diffusion is decreased as the hydrided region grows, since the expansion of the hydride formation produces a reduction in the stresses at the crack tip [3]. According to Metzger *et al.* [3], the stress drop per increment of hydride growth becomes increasingly more significant as K_I decreases. Thus, the stress-drop effect is very important in the region of K_{IH}. Therefore, one sees that hydride growth can be a self-limiting process. This cessation will not occur of course if the hydride growth is truncated by a fracture event, which restarts the growth at a new crack tip.

The critical lengths for hydride fracture, as described by the solid line, were predicted by both the critical stress model [2] and the energy balance model [4]. But here in considering the fracture of the hydride cluster, we should consider the fracture of both hydrides and

ductile matrix ligaments, because a hydride cluster consists of both hydrides and matrix ligaments [11–13].

According to Fig. 3, one can see that fracture can only begin to occur when the curve for the length of maximum growth and the curve for the critical length for fracture intersect. This explains the threshold phenomenon for delayed hydride cracking.

The hydride cluster lengths measured in this work were compared with the results of theoretical work [2, 4, 5]. In Fig. 3, we found the dotted-line fits the relation $L \propto K_I^2$, which agrees with the prediction in [2]. The Equation 15 in [2] can be written as:

$$L_{\max} = \frac{1}{2\pi}\left[\frac{\bar{V}_H}{RT}\frac{2(1+\nu)K_I}{3\ln(C^p/C_0)}\right]^2, \qquad (1)$$

where $L_{\max}$ is the maximum hydride length, $\bar{V}_H = 1.67 \times 10^{-6}$ m^3/mol is the partial molal volume of hydrogen in zirconium [14, 15], $R = 8.314$ J/mol·K the gas constant, T the temperature in Kelvin, $\nu = 0.329$ the Poisson's ratio, and K_I the stress intensity factor. C^p and C_0 are the hydrogen concentration for precipitation and the initial hydrogen concentration in solution in the specimen, respectively. Equation 1 generally predicts the same dependency of hydride cluster length on the stress intensity as we experimentally measured. If we further use this equation as the theoretical approximation to our experimental conditions, then by fitting the equation to the dotted-line in Fig. 3 we get $C^p/C_0 = 1.223$ for 150°C, which defines the hydrogen distribution at the hydride growth limit.

In comparing the critical length for hydride fracture, we use Equation 8 based on reference [4], which gives an explicit relation between the critical hydride length L_c and K_I. Zheng *et al*.'s equation 8 can be rewritten as:

$$G_c = \frac{1.556L_c}{1.556L_c + K_I^2/(6\pi\sigma_y^2)}\frac{1-\nu^2}{E}K_I^2, \qquad (2)$$

where G_c is the *specific* "energy required to create the fracture surface", L_c is the critical hydride cluster length, and K_I is the applied stress intensity factor. From [4], the Young's modulus $E = 81.541$ GPa, and the Poisson's ratio $\nu = 0.329$. The measured yield stress of the Zr-2.5wt% Nb alloy used in this work was 630 MPa at 150°C (see Table II). In Fig. 5, the critical lengths for hydride fracture given by the solid line in Fig. 3 are compared with the above Equation 1 from [4]. The experimental results show a similar dependency on K_I as predicted by theoretical work [2, 4]. A difference is that in the theoretical work [2, 4], a much steeper (almost vertical) increase was predicted in the critical length of hydride cluster when K_I drops to near K_{IH}. However, for our experimentally measured critical length, although the change is also rapid, it is not as abrupt, as shown in Fig. 5. This is because in those theoretical works, the energy G_c (or the stress) required to create the fracture surface was taken as a constant, while in real experiments, this energy actually is a variable and decreases with the increasing length of the hydride cluster. This point was examined by Zheng *et al*. in a later analysis [5] and they showed by consideration of striation lengths that G_c decreases as the hydride length increases. Our present results confirm that analysis.

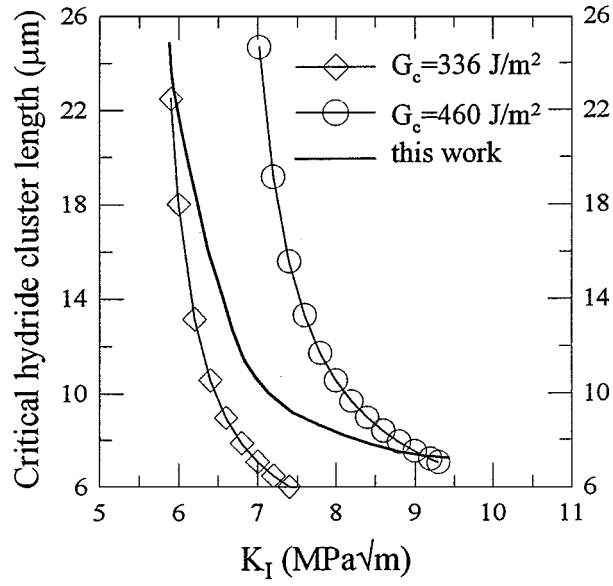

Figure 5 Comparison of experimental data from this work with existing theoretical work (Equation 8 from reference [4]).

In this work, the lengths of hydride clusters were measured at a depth of about 0.1 mm from the side surface. These lengths are taken as representative of the hydride length across the plane strain region at the crack front. This is justified since for the K_I range in which we did our experiments, the variation of crack length across the specimen thickness is small, except possible right at the surface in the region of plane stress.

5. Conclusions

(1) A modified experimental method has been developed in this work, by which individual hydride clusters formed and fractured at crack tips can be observed and studied one by one. This method is particularly useful for $K_I < K_{IH}$ or $K_I > K_{IH}$ but near K_{IH}.

(2) Using this method, wedge-shaped hydride clusters were observed, which confirmed the theoretical prediction by Metzger *et al*. [3].

(3) The limit for hydride growth was determined for $K_I < K_{IH}$. The maximum length for hydride growth was found to increase with K_I and be proportional to K_I^2, in agreement with existing theoretical work.

(4) The critical length of the hydride cluster that could be fractured at the crack tip was determined for $K_I > K_{IH}$ but near K_{IH}. The critical hydride cluster length showed a similar but more gradual dependency on K_I than that predicted by the theoretical work. This confirms that the energy required to create the fracture surface through the hydride cluster is a variable and decreases as K_I decreases.

Acknowledgement

This work was partially funded by NSERC. The authors are also grateful to CRL-AECL for providing the alloy used in this work.

References

1. R. DUTTON, K. NUTTALL, M. P. PULS and L. A. SIMPSON, *Metall. Trans.* **8A** (1977) 1553.
2. S. SHI and M. P. PULS, *J. Nucl. Mat.* **218** (1994) 30.
3. D. R. METZGER and R. G. SAUVÉ, PVP, Vol. 326 (Computer Technology: Application and Methodology, ASME 1996) p. 137.
4. X. J. ZHENG, L. LUO, D. R. METZGER and R. G. SAUVÉ, *J. Nucl. Mat.* **218** (1995) 174.
5. X. J. ZHENG, D. R. METZGER, G. GLINKA and R. N. DUBEY, PVP, Vol. 326 (Computer Technology: Application and Methodology, ASME 1996) p. 181.
6. R. DUTTON, C. H. WOO, K. NUTTALL, L. A. SIMPSON and M. P. PULS, "Hydrogen in Metals" (Pergamon, Oxford, 1978) Paper 3C6.
7. K. F. AMOUZOUVI and L. J. CLEGG, in Proceedings of the International Symposium on Fracture Mechanics, Winnipeg, Canada, August 1987, edited by W. R. Tyson and B. Mukherjee (Pergamon, Oxford, 1988) p. 107.
8. S. SAGAT, S. Q. SHI and M. P. PULS, *Mat. Sci. and Eng.* **A176** (1994) 237.
9. M. LEGER and O. KIIR, Ontario Hydro Research Division Report 80-303-K, August 29 (1980).
10. G. LIN, S. SKRZYPEK, D. LI and R. L. EADIE, *J. Testing and Evaluation* **26** (1998) 15.
11. E. SMITH, *J. Mat. Sci.* **30** (1995) 5910.
12. *Idem., Int. J. Pres. Ves. & Piping* **61** (1995) 1.
13. G. SHEK, M. T. JOVANOVIC, H. SEAHRA, Y. MA, D. LI and R. L. EADIE, *J. Nucl. Mater.* **231** (1996) 221.
14. S. R. MACEWEN, C. E. COLEMAN, C. E. ELLS and J. FABER, JR., *Acta Metall.* **33** (1985) 753.
15. R. L. EADIE, T. TASHIRO, D. HARRINGTON and M. LEGER, *Scripta Metall. et. Mat.* **26** (1992) 231.

Received 28 May
and accepted 31 December 1999